

# SiOC thin films: an efficient light source and an ideal host matrix for $\text{Eu}^{2+}$ ions

Gabriele Bellocchi,<sup>1,2</sup> Fabio Iacona,<sup>1,\*</sup> Maria Miritello,<sup>1</sup>  
Tiziana Cesca,<sup>3</sup> and Giorgia Franzò<sup>1</sup>

<sup>1</sup>MATIS IMM CNR, Via Santa Sofia 64, 95123 Catania, Italy

<sup>2</sup>Dipartimento di Fisica e Astronomia, Università di Catania, Via Santa Sofia 64, 95123 Catania, Italy

<sup>3</sup>Dipartimento di Fisica e Astronomia, Università di Padova, Via F. Marzolo 8, 35131 Padova, Italy  
[\\*fabio.iacona@ct.infn.it](mailto:fabio.iacona@ct.infn.it)

**Abstract:** The intense luminescence of SiOC layers is studied and its dependence on the parameters of the thermal annealing process elucidated. Although the emission of SiOC is bright enough to be interesting for practical applications, this material is even more promising as a host matrix for optically active Eu ions. Indeed, when incorporated in a SiOC matrix,  $\text{Eu}^{3+}$  ions are efficiently reduced to  $\text{Eu}^{2+}$ , producing a very strong visible luminescence peaked at 440 nm.  $\text{Eu}^{2+}$  ions benefit also of the occurrence of an energy transfer mechanism involving the matrix, which increases the efficiency of photon absorption for exciting wavelengths shorter than 300 nm. We evaluate that Eu doping of SiOC produces an enhancement of the luminescence intensity at 440 nm accounting for about a factor of 15. These properties open the way to new promising perspectives for the application of Eu-doped materials in photonic and lighting technologies.

©2013 Optical Society of America

**OCIS codes:** (260.3800) Luminescence; (160.4670) Optical materials; (160.5690) Rare-earth-doped materials.

---

## References and links

1. L. Pavesi, L. Dal Negro, C. Mazzoleni, G. Franzò, and F. Priolo, "Optical gain in silicon nanocrystals," *Nature* **408**(6811), 440–444 (2000).
2. G. Franzò, V. Vinciguerra, and F. Priolo, "The excitation mechanism of rare-earth ions in silicon nanocrystals," *Appl. Phys., A Mater. Sci. Process.* **69**(1), 3–12 (1999).
3. M. Fujii, M. Yoshida, Y. Kanzawa, S. Hayashi, and K. Yamamoto, "1.54  $\mu\text{m}$  photoluminescence of  $\text{Er}^{3+}$  doped into  $\text{SiO}_2$  films containing Si nanocrystals: Evidence for energy transfer from Si nanocrystals to  $\text{Er}^{3+}$ ," *Appl. Phys. Lett.* **71**(9), 1198–1200 (1997).
4. J. H. Shin, J. Lee, H.-S. Han, J.-H. Jhe, J. S. Chang, S.-Y. Seo, H. Lee, and N. Park, "Si nanocluster sensitization of Er-doped silica for optical amplet using top-pumping visible LEDs," *IEEE J. Sel. Top. Quantum Electron.* **12**(4), 783–796 (2006).
5. X. Ye, W. Zhuang, Y. Hu, T. He, X. Huang, C. Liao, S. Zhong, Z. Xu, H. Nie, and G. Deng, "Preparation, characterization, and optical properties of nano- and submicron-sized  $\text{Y}_2\text{O}_3:\text{Eu}^{3+}$  phosphors," *J. Appl. Phys.* **105**(6), 064302 (2009).
6. D. Li, X. Zhang, L. Jin, and D. Yang, "Structure and luminescence evolution of annealed europium-doped silicon oxides films," *Opt. Express* **18**(26), 27191–27196 (2010).
7. L. Rebohle, J. Lehmann, S. Prucnal, A. Kanjilal, A. Nazarov, I. Tyagulskii, W. Skorupa, and M. Helm, "Blue and red electroluminescence of Europium-implanted metal-oxide-semiconductor structures as a probe for the dynamics of microstructure," *Appl. Phys. Lett.* **93**(7), 071908 (2008).
8. L. Rebohle, J. Lehmann, S. Prucnal, A. Nazarov, I. Tyagulskii, S. Tyagulskii, A. Kanjilal, M. Voelskow, D. Grambole, W. Skorupa, and M. Helm, "Anomalous wear-out phenomena of europium-implanted light emitters based on a metal-oxide-semiconductor structure," *J. Appl. Phys.* **106**(12), 123103 (2009).
9. S. Prucnal, J. M. Sun, W. Skorupa, and M. Helm, "Switchable two-color electroluminescence based on a Si metal-oxide-semiconductor structure doped with Eu," *Appl. Phys. Lett.* **90**(18), 181121 (2007).
10. N. D. Afify and G. Mountjoy, "Molecular-dynamics modeling of  $\text{Eu}^{3+}$ -ion clustering in  $\text{SiO}_2$  glass," *Phys. Rev. B* **79**(2), 024202 (2009).
11. J. Laegsgaard, "Theory of  $\text{Al}_2\text{O}_3$  incorporation in  $\text{SiO}_2$ ," *Phys. Rev. B* **65**(17), 174104 (2002).
12. S. Boninelli, G. Bellocchi, G. Franzò, M. Miritello, and F. Iacona, "New strategies to improve the luminescence efficiency of Eu ions embedded in Si-based matrices," *J. Appl. Phys.* **113**(14), 143503 (2013).

13. J. Qi, T. Matsumoto, M. Tanaka, and Y. Masumoto, "Electroluminescence of europium silicate thin film on silicon," *Appl. Phys. Lett.* **74**(21), 3203–3205 (1999).
14. Y. C. Shin, D. H. Kong, W. C. Choi, and T. G. Kim, "Formation of europium-silicate thin films and their photoluminescence properties," *J. Korean Phys. Soc.* **48**, 1246–1249 (2006).
15. Y. C. Shin, S. J. Leem, C. M. Kim, S. J. Kim, Y. M. Sung, C. K. Hahn, J. H. Baek, and T. G. Kim, "Deposition of europium oxide on Si and its optical properties depending on thermal annealing conditions," *J. Electroceram.* **23**(2-4), 326–330 (2009).
16. G. Bellocchi, G. Franzò, F. Iacona, S. Boninelli, M. Miritello, T. Cesca, and F. Priolo, "Eu<sup>3+</sup> reduction and efficient light emission in Eu<sub>2</sub>O<sub>3</sub> films deposited on Si substrates," *Opt. Express* **20**(5), 5501–5507 (2012).
17. S.-Y. Seo, K.-S. Cho, and J. H. Shin, "Intense blue-white luminescence from carbon-doped silicon-rich silicon oxide," *Appl. Phys. Lett.* **84**(5), 717–719 (2004).
18. S. Gallis, V. Nikas, H. Suhag, M. Huang, and A. E. Kaloyeros, "White light emission from amorphous silicon oxycarbide (a-SiC<sub>x</sub>O<sub>y</sub>) thin films: Role of composition and postdeposition annealing," *Appl. Phys. Lett.* **97**(8), 081905 (2010).
19. Y. P. Guo, J. C. Zheng, A. T. S. Wee, C. H. A. Huan, K. Li, J. S. Pan, Z. C. Feng, and S. J. Chua, "Photoluminescence studies of SiC nanocrystals embedded in a SiO<sub>2</sub> matrix," *Chem. Phys. Lett.* **339**(5-6), 319–322 (2001).
20. A. Perez-Rodriguez, O. Gonzalez-Varona, B. Garrido, P. Pellegrino, J. R. Morante, C. Bonafos, M. Carrada, and A. Claverie, "White luminescence from Si<sup>-</sup> and C<sup>+</sup> ion-implanted SiO<sub>2</sub> films," *J. Appl. Phys.* **94**(1), 254–262 (2003).
21. Y. Ishikawa, A. V. Vasin, J. Salonen, S. Muto, V. S. Lysenko, A. N. Nazarov, N. Shibata, and V.-P. Lehto, "Color control of white photoluminescence from carbon-incorporated silicon oxide," *J. Appl. Phys.* **104**(8), 083522 (2008).
22. Y. Ding and H. Shirai, "White light emission from silicon oxycarbide films prepared by using atmospheric pressure microplasma jet," *J. Appl. Phys.* **105**(4), 043515 (2009).
23. A. V. Vasin, Y. Ishikawa, N. Shibata, J. Salonen, and V.-P. Lehto, "Strong white photoluminescence from carbon-incorporated silicon oxide fabricated by preferential oxidation of silicon in nano-structured Si:C layer," *Jpn. J. Appl. Phys.* **46**(19), L465–L467 (2007).
24. S. Gallis, M. Huang, and A. E. Kaloyeros, "Efficient energy transfer from silicon oxycarbide matrix to Er ions via indirect excitation mechanisms," *Appl. Phys. Lett.* **90**(16), 161914 (2007).
25. Y. Zhang, A. Quaranta, and G. D. Soraru, "Synthesis and luminescent properties of novel Eu<sup>2+</sup>-doped silicon oxycarbide glasses," *Opt. Mater.* **24**(4), 601–605 (2004).
26. G. Blasse and B. C. Grabmaier, *Luminescent Materials* (Springer Verlag, 1994).
27. X. Song, R. Fu, S. Agathopoulos, H. He, X. Zhao, and S. Zhang, "Photoluminescence properties of Eu<sup>2+</sup>-activated CaSi<sub>2</sub>O<sub>2</sub>N<sub>2</sub>: Redshift and concentration quenching," *J. Appl. Phys.* **106**(3), 033103 (2009).
28. C. M. Brewer, D. R. Bujalski, V. E. Parent, K. Su, and G. A. Zank, "Insights into the oxidation chemistry of SiOC ceramics derived from silsesquioxanes," *J. Sol-Gel Sci. Technol.* **14**(1), 49–68 (1999).
29. T. Rajagopalan, X. Wang, B. Lahlouh, C. Ramkumar, P. Dutta, and S. Gangopadhyaya, "Low temperature deposition of nanocrystalline silicon carbide films by plasma enhanced chemical vapor deposition and their structural and optical characterization," *J. Appl. Phys.* **94**(8), 5252–5260 (2003).
30. J. Y. Kim, M. S. Hwang, Y.-H. Kim, H. J. Kim, and Y. Lee, "Origin of low dielectric constant of carbon-incorporated silicon oxide film deposited by plasma enhanced chemical vapor deposition," *J. Appl. Phys.* **90**(5), 2469–2473 (2001).
31. Q. Zhang, X. Liu, Y. Qiao, B. Qian, G. Dong, J. Ruan, Q. Zhou, J. Qiu, and D. Chen, "Reduction of Eu<sup>3+</sup> to Eu<sup>2+</sup> in Eu-doped high silica glass prepared in air atmosphere," *Opt. Mater.* **32**(3), 427–431 (2010).
32. Y. Kishimoto, X. Zhang, T. Hayakawa, and M. Nogami, "Blue light emission from Eu<sup>2+</sup> ions in sol-gel-derived Al<sub>2</sub>O<sub>3</sub>-SiO<sub>2</sub> glasses," *J. Lumin.* **129**(9), 1055–1059 (2009).
33. Y. Qiao, D. Chen, J. Ren, B. Wu, J. Qiu, and T. Akai, "Blue emission from Eu<sup>2+</sup>-doped high silica glass by near-infrared femtosecond laser irradiation," *J. Appl. Phys.* **103**(2), 023108 (2008).
34. J. Linnros, N. Lalic, A. Galeckas, and V. Grivickas, "Analysis of the stretched exponential photoluminescence decay from nanometer-sized silicon crystals in SiO<sub>2</sub>," *J. Appl. Phys.* **86**(11), 6128–6134 (1999).

## 1. Introduction

The realization of an efficient Si-based light source represents one of the most relevant issues for the scientific community currently working in the field of photonics. The main characteristics required for this source are high efficiency at room temperature, tunability in a wide wavelength range, easy integration in highly compact Si microphotonic devices. In this framework, during the last decade, the bright light emission provided by Si nanocrystals (nc) embedded in a SiO<sub>2</sub> matrix has gathered a lot of interest [1]. A leading role in the field of Si photonics is also played by rare earth (RE) ions; RE doping of insulating or semiconducting host matrices has been recognized as a powerful method to provide intense luminescence signals spanning in a wide wavelength range, opening the way to several new applications for

Si-based materials in the field of photonics [2]. A relevant example of this approach is represented by the very intense 1.54  $\mu\text{m}$  luminescence provided by Er-doped Si nc [3], which has opened new perspectives for the fabrication of Si-based optical amplifiers [4]. Among the other RE ions, a considerable attention has been devoted to Eu. Both divalent and trivalent Eu ions can act as efficient emitting centers in the visible region and their bright emission is widely employed in phosphors used in plasma display panels and in solid state lighting [5]. On the other hand, applications of Eu in Si photonics require the availability of Eu-containing thin films compatible with CMOS technology. Several papers have studied the optical properties of Eu-doped SiO<sub>2</sub> films [6–9], but the very low Eu solid solubility in silica (cluster formation occurs for Eu concentrations larger than  $10^{18} \text{ cm}^{-3}$  [10–12]) seems to seriously limit its perspectives in photonics. As an interesting alternative approach to doping, also Eu compound thin films have received a considerable attention [13–16].

A different approach to obtain efficient light emission from a Si-based material is represented by Si oxycarbide (SiOC), which has been extensively studied for its intense photoluminescence (PL) emission in the visible range [17–23]. PL emission from SiOC films generally consists of multiple contributions, which have been attributed to different centers, including Si-C bonds in C-containing Si (or SiC) nanoclusters [17,20], C- and Si-related O defects [18,21], defects at the SiC/SiO<sub>2</sub> interface [19], neutral oxygen vacancies [22]. Furthermore, it has been also evidenced that SiOC can be an interesting host material for RE ions, including Er [24] and Eu [12,25]. Indeed, under suitable experimental conditions, Eu ions have a remarkably higher solid solubility in SiOC than in SiO<sub>2</sub> [12]. In addition, in a SiOC matrix the formation of Eu<sup>2+</sup> ions, which exhibit a very strong emission originating from dipole-allowed  $4f^65d \rightarrow 4f^7$  transitions, is favorite with respect to that of Eu<sup>3+</sup> ions, whose intra 4f-shell transition, being dipole-forbidden, leads to a less intense luminescence [26]. A further appealing feature of the emission of Eu<sup>2+</sup> ions is the possibility to tune the PL peak position in a wide range within the visible region by changing the Eu concentration [27].

In this paper we will study the optical properties of SiOC and Eu-doped SiOC thin films synthesized by rf magnetron sputtering. It will be demonstrated that the temperature and the environment of the thermal annealing process have a key role in determining the features of the PL emission in the visible region from both materials. The mechanisms of the SiOC-Eu interaction, leading to a very bright visible emission assigned to Eu<sup>2+</sup> ions, will be also elucidated. The relevance of the above data for the realization of an efficient Si-based light source, which can be of great interest for applications in photonics as well as in solid state lighting, will be addressed.

## 2. Experimental section

SiOC and Eu-doped SiOC thin films have been synthesized by using an UHV rf magnetron sputtering system. The chamber base pressure was about  $1 \times 10^{-9}$  mbar. The deposition has been obtained by co-sputtering of 4-inches diameter, water-cooled SiO<sub>2</sub> and SiC targets (in the case of SiOC samples), and SiO<sub>2</sub>, SiC and Eu<sub>2</sub>O<sub>3</sub> targets (in the case of Eu-doped SiOC samples). C concentration has been fixed at about 5 at.% in both doped and undoped SiOC films, while Eu concentration was  $1.5 \times 10^{20} \text{ cm}^{-3}$ . The films were deposited on Si substrates kept at 400 °C in a  $5 \times 10^{-3}$  mbar Ar atmosphere. After deposition the films were thermally treated at temperatures ranging from 600 to 900 °C for 1 h in O<sub>2</sub> or N<sub>2</sub> atmosphere.

Both doped and undoped as-deposited SiOC films are about 190 nm thick, as measured by both ellipsometry and cross sectional transmission electron microscopy. The refractive index of SiOC samples was measured using an ellipsometer equipped with a He-Ne laser operating at 632.8 nm. The Eu content of the film was determined by Rutherford backscattering spectrometry measurements, performed by using a 2 MeV He<sup>+</sup> beam, with the detector placed at an angle of 165° with respect to the incident beam.

PL measurements were performed by pumping with the 325 nm line of a He-Cd laser. The pump power was about 3 mW and the laser beam was chopped through an acousto-optic

modulator at a frequency of 55 Hz. The PL signal was analyzed by a single grating monochromator and detected with a Hamamatsu visible photomultiplier. Spectra were recorded with a lock-in amplifier using the acousto-optic modulator frequency as a reference. The same experimental set-up has been maintained for PL measurements of both undoped and Eu-doped films, in order to allow the direct comparison of the intensities. PL lifetime measurements were performed by monitoring the decay of the luminescence signal at a fixed wavelength after pumping to steady state and switching off the laser beam. The overall time resolution of our system is of 200 ns.

Photoluminescence excitation (PLE) measurements in the 250-475 nm range were performed by using a FluoroMax spectrofluorometer by Horiba. All the spectra have been measured at room temperature and corrected for the system spectral response.

### 3. Results and discussion

The room temperature PL spectra of as-deposited and thermally annealed SiOC films, obtained by exciting with the 325 nm line of a He-Cd laser, are shown in Fig. 1; Figs. 1(a) and 1(b) refer to samples annealed in N<sub>2</sub> and O<sub>2</sub> atmosphere, respectively, the explored temperature range is 600-900 °C and the duration of all the processes is 1 h.

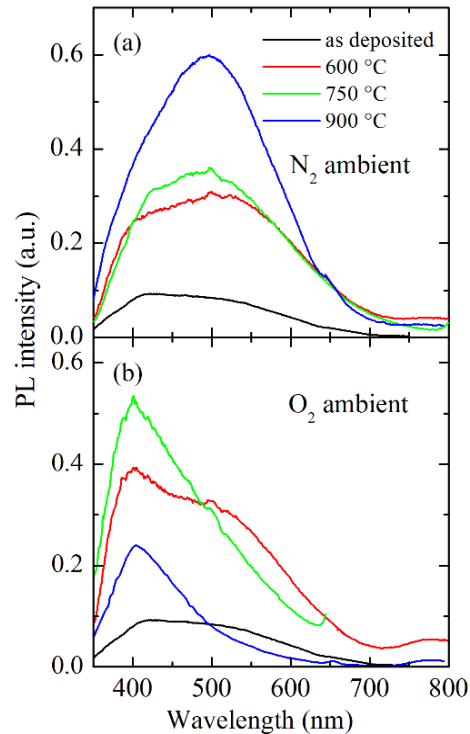


Fig. 1. Room temperature PL spectra for SiOC films as deposited and annealed in the temperature range 600 – 900 °C (a) for 1h in N<sub>2</sub> ambient, and (b) in O<sub>2</sub> ambient.

It is noteworthy that all PL signals shown in the figure are visible by the naked eye. Furthermore, it is evident that the conditions of the thermal treatment strongly influence the optical properties of the films; in particular, both the intensity and the shape of the PL peaks markedly depend on the ambient and on the temperature of the thermal process. More in detail, spectra of O<sub>2</sub>-annealed samples are generally blueshifted and sharper with respect to those of samples annealed in N<sub>2</sub> and the PL signal is maximized at 900 °C for processes performed in N<sub>2</sub> and at 750 °C for processes performed in O<sub>2</sub>.

In order to gain deeper information about the nature of the observed PL emission, in Fig. 2 we compare the PL spectrum of an as-deposited film (black line) with those measured in samples annealed in N<sub>2</sub> (red line) or O<sub>2</sub> (blue line) ambient at the same temperature of 900 °C. All spectra have been normalized to allow an easier comparison. The spectrum of the as-deposited sample appears quite broad, suggesting the presence of at least two different contributions originating from two different luminescent centers. The complex nature of the PL emission of SiOC films can be better understood by analyzing the PL peaks of the annealed films. Indeed, after annealing in N<sub>2</sub> atmosphere, a peak at 510 nm becomes predominant, although it is still visible a shoulder at 400 nm. In contrast, after annealing in O<sub>2</sub> atmosphere, the maximum of the band is found at 400 nm and the component at 510 nm is almost completely quenched.

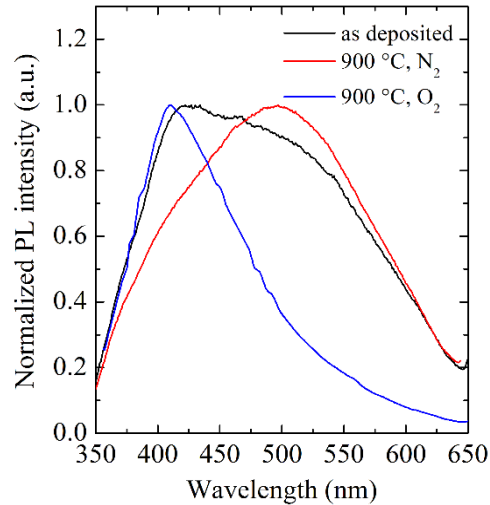


Fig. 2. Comparison between the normalized PL spectra of SiOC films as deposited and annealed at 900 °C in N<sub>2</sub> and in O<sub>2</sub> ambient.

The behavior of the two components of the PL emission of SiOC films as a function of the annealing temperature for both N<sub>2</sub> and O<sub>2</sub> processes can be analyzed by plotting their integrated intensity, obtained by a suitable fitting procedure employing Gaussian peaks. These data are reported in Fig. 3; for processes performed in N<sub>2</sub> atmosphere (Fig. 3(a)) the prevalent PL band is the one at 510 nm and its intensity (plotted as red line and circles) continuously increases by increasing the annealing temperature, while the intensity of the component at 400 nm (blue line and circles) remains quite low and almost constant throughout the explored temperature range. In contrast, for samples annealed in O<sub>2</sub> atmosphere (Fig. 3(b)), the prevalent PL band is the one at 400 nm and its intensity has a maximum at 750 °C and decreases at higher temperatures, while the component at 510 nm has a maximum at 600 °C and decreases at higher temperatures, being almost completely quenched at 900 °C.

In order to obtain more information on the nature of the two luminescent centers, we have performed PLE spectroscopy measurements on SiOC samples annealed at 900 °C. The PLE intensity shown in Fig. 4, obtained by integrating the emission spectra recorded as a function of the excitation wavelength in the range 250-370 nm, is deeply influenced by the annealing environment. In particular, for the sample annealed in N<sub>2</sub>, the integral PL intensity is almost constant between 250 and 270 nm and then steeply drops by increasing the excitation wavelength, while for the sample annealed in O<sub>2</sub> it monotonically decreases with increasing wavelength.

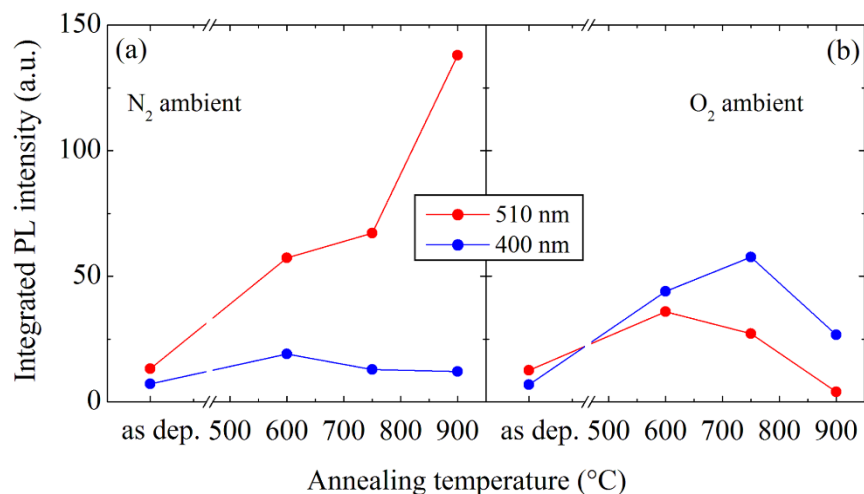


Fig. 3. Integrated intensity as a function of the annealing temperature for the two components of the PL signal of SiOC films annealed (a) in N<sub>2</sub> ambient, and (b) in O<sub>2</sub> ambient. The red circles refer to the component at 510 nm, the blue ones to the component at 400 nm.

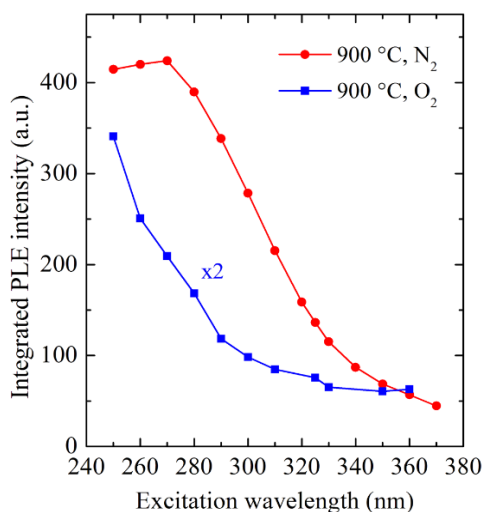


Fig. 4. Room temperature PLE intensity obtained by integrating the PL spectra recorded as a function of the excitation wavelength in the range 250-370 nm for SiOC films annealed at 900 °C in N<sub>2</sub> (red circles and line), and O<sub>2</sub> (blue squares and line, multiplied by a factor of 2).

On the basis of the data shown in Figs. 1-4 it is possible to reasonably conclude that the peak at 510 nm is due to the presence of Si-C bonds [17,20], while the peak at 400 nm can be assigned to luminescent defects, such as oxygen vacancies [18,21,22]. Indeed, when SiOC films are annealed in N<sub>2</sub> atmosphere, a partial ordering of the film structure occurs, leading to the formation of optically active Si-C bonds; in agreement with this picture, the increase of the PL signal at 510 nm as a function of the annealing temperature for N<sub>2</sub> processes, shown in Fig. 3(a), is due to the increment of the concentration of these bonds. The evidence that the system becomes more optically efficient at higher temperatures confirms that the PL at 510 nm cannot be assigned to defect centers, further supporting its assignment to Si-C bonds. On the other hand, by increasing the annealing temperature of O<sub>2</sub>-treated samples, Si-C bonds emission intensity decreases because the oxidation of SiOC films implies a decrease of the C concentration into the film.

As far as the component at 400 nm is concerned, the oxygen vacancies responsible of this emission are already present in the as-deposited material and their concentration is not strongly affected by annealing processes in  $N_2$ . On the other hand, as expected, their concentration remarkably increases during the annealing in  $O_2$  ambient, due to the elimination of C atoms through the formation of volatile species such as CO or  $CO_2$  [28], and decreases at higher annealing temperature, due to the recovery of the chemical luminescent defects of the film induced by the thermal treatment, leading to the formation of a nearly stoichiometric  $SiO_2$  layer.

A confirmation of the above picture concerning the nature of the PL emission in SiOC films has been obtained by ellipsometric measurements of the refractive index at 632.8 nm. Figure 5 shows the evolution of the refractive index as a function of the annealing temperature for SiOC films treated in  $N_2$  or  $O_2$  ambient.

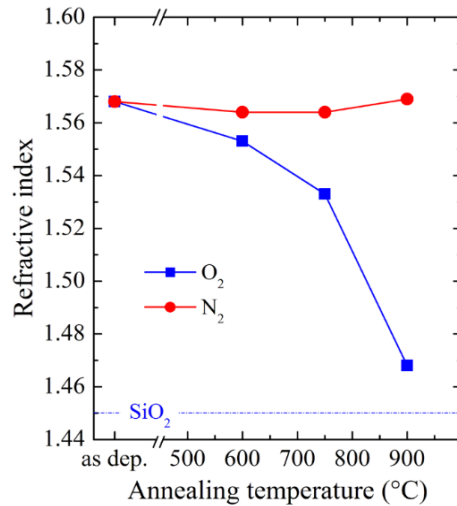


Fig. 5. Refractive index, measured at 632.8 nm, as a function of the annealing temperature for SiOC films annealed in  $N_2$  (red circles and line), and  $O_2$  (blue squares and line). The refractive index of pure  $SiO_2$  is indicated by a blue dash-dotted line.

The as-deposited sample has a refractive index of about 1.57, which reflects its low C content (pure SiC refractive index is about 2.60 [29], while pure  $SiO_2$  refractive index is about 1.45 [30]). For annealing in  $N_2$  atmosphere (red line and circles), the refractive index is almost constant throughout the explored temperature range (from room temperature up to 900 °C), indicating that the stoichiometry does not change during the annealing process, in agreement with the conclusions drawn on the basis of the above discussed PL data. In contrast, after annealing in  $O_2$  atmosphere (blue line and squares), the refractive index decreases with increasing the annealing temperature. This corresponds to a change in the sample stoichiometry, and in particular to a variation of the C content in the  $SiO_2$  matrix. Indeed the annealing process in oxidizing ambient induces the diffusion of oxygen inside the sample and its reaction with the C contained into the SiOC film, leading to the formation of small gaseous molecules such as CO or  $CO_2$  which can therefore escape from the sample, leaving it depleted in C and oxidized [28]. With increasing temperature, oxidation rate increases too, and the final result is a deep change of the stoichiometry of SiOC samples, leading to a continuous reduction of the refractive index, towards the typical  $SiO_2$  value (1.45), indicated in Fig. 5 by a dash-dotted blue line. The variation of the refractive index of SiOC films annealed in  $O_2$  is in full agreement with the optical properties described in Figs. 1-4.

As previously reported [12,25], SiOC can be also a very suitable host matrix for luminescent Eu ions. Indeed, Eu precipitation, which strongly limits the optical efficiency of Eu ions embedded in the more conventional SiO<sub>2</sub> matrix, can be almost completely suppressed in SiOC. Furthermore, SiOC is also able to induce the Eu<sup>3+</sup> → Eu<sup>2+</sup> reduction, providing a simple method to obtain high concentrations of the most optically efficient Eu species (Eu<sup>2+</sup>). Figure 6 reports the room temperature PL spectra, obtained by exciting with the 325 nm line of a He-Cd laser, of Eu-doped SiOC samples having an Eu concentration of 1.5 × 10<sup>20</sup> cm<sup>-3</sup>, treated at 900 °C in N<sub>2</sub> or O<sub>2</sub> ambient. The N<sub>2</sub>-treated sample (blue line) exhibits a very intense PL band, centered at about 440 nm, due to the 4f<sup>6</sup>5d → 4f<sup>7</sup> transitions of Eu<sup>2+</sup> ions, massively formed owing to a reduction reaction involving the C atoms of the SiOC matrix [12]. No PL lines associated to Eu<sup>3+</sup> are detected. The PL spectrum of the sample treated in O<sub>2</sub> ambient (magenta line, multiplied by a factor of 10 in the region 370-550 nm and by a factor of 400 in the region 550-750 nm) shows a band centered at about 420 nm, attributable to Eu<sup>2+</sup> ions, and some weaker sharp peaks at longer wavelengths, typical of Eu<sup>3+</sup> emission; the main Eu<sup>3+</sup> peak is detected at 618 nm, which corresponds to the <sup>5</sup>D<sub>0</sub> → <sup>7</sup>F<sub>2</sub> transition. The other less intense peaks at about 575, 657, and 705 nm correspond to <sup>5</sup>D<sub>0</sub> → <sup>7</sup>F<sub>J</sub> transitions of Eu<sup>3+</sup> ions in solid matrices, with J = 0, 3 and 5, respectively. As expected, the annealing in oxidizing ambient promotes the formation of Eu<sup>3+</sup> ions and it is therefore unsuitable to provide a strong Eu<sup>2+</sup> emission. The shift of about 20 nm between the Eu<sup>2+</sup> peaks detected in SiOC films annealed in O<sub>2</sub> or N<sub>2</sub> ambient is due to the well known dependence of the wavelength of this emission on the Eu concentration [27].

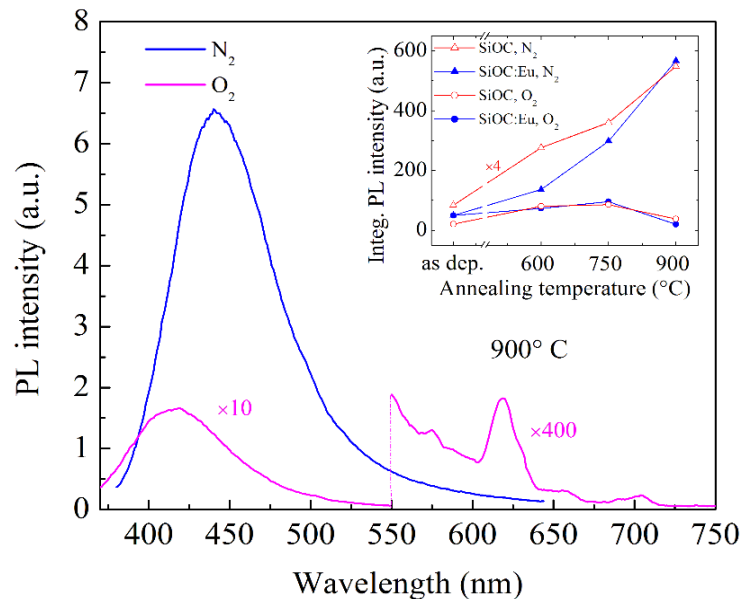


Fig. 6. Room temperature PL spectra for Eu-doped SiOC films annealed at 900 °C in N<sub>2</sub> (blue line), and in O<sub>2</sub> ambient (magenta line, multiplied by a factor of 10 in the region 370-550 nm and by a factor of 400 in the region 550-750 nm). Eu concentration is 1.5 × 10<sup>20</sup> cm<sup>-3</sup>. The inset compares the integrated PL intensity as a function of the annealing temperature of undoped and Eu-doped SiOC (for both processes in N<sub>2</sub> and O<sub>2</sub>); the data referring to undoped SiOC annealed in N<sub>2</sub> are multiplied by a factor of 4 to allow an easier comparison.

No relevant variation of the wavelength and of the width of the PL peaks of Eu-doped SiOC is found by varying the temperature of the annealing process in N<sub>2</sub> or in O<sub>2</sub>; on the other hand, the intensity of the PL signals depends on the annealing temperature, as shown in the inset of Fig. 6. For Eu-doped SiOC samples treated in N<sub>2</sub> (blue closed triangles) a monotonic increase of the integrated PL intensity as a function of the annealing temperature is



found, while only a weak dependence is observed for processes in O<sub>2</sub> (blue closed circles). Interestingly, these trends are very similar to those obtained by analyzing undoped SiOC samples after the same thermal processes, as shown in the inset of Fig. 6 (red open triangles refer to processes in N<sub>2</sub>, red open circles to processes in O<sub>2</sub>). The PL intensity values for undoped SiOC films treated in N<sub>2</sub> are remarkably weaker than those relative to the doped samples, so that they have been multiplied by a factor of 4, to make easier the comparison with the data relative to the doped films. The overlap between the trends of the PL intensity as a function of temperature for undoped and Eu-doped SiOC annealed in N<sub>2</sub> is due to the fact that Eu<sup>2+</sup> ions (which are by far the Eu species giving the main contribution to the PL signal of Eu-doped SiOC films) are formed owing to a redox reaction involving Eu<sup>3+</sup> ions and Si-C bonds (which, as described in Fig. 3, give the main contribution to the PL signal of undoped SiOC films annealed in N<sub>2</sub>). Indeed, by increasing the annealing temperature, the concentration of Si-C bonds increases and, as a consequence, the number of emitting Eu<sup>2+</sup> ions, formed through the redox reaction, becomes higher. A confirmation of the above mechanism is given by the behavior of the samples annealed in O<sub>2</sub> environment. As demonstrated by Figs. 3 and 5, O<sub>2</sub> strongly decreases the content of Si-C bonds in the SiOC films, leading to a PL emission which is dominated by radiative defects; as a consequence, Eu<sup>2+</sup> ions formation in Eu-doped films is strongly inhibited, and only a weak PL signal is obtained. The inset of Fig. 6 evidences a very steep increase of the PL intensity of Eu-doped films by increasing the annealing temperature in N<sub>2</sub> ambient. This implies an enhancement of the luminescence intensity at 440 nm (in correspondence to the Eu peak emission) in Eu-doped samples with respect to the undoped ones which accounts for about a factor of 15 for an annealing temperature of 900 °C.

Figure 7 reports the room temperature PLE spectrum of Eu-doped SiOC with an Eu concentration of  $1.5 \times 10^{20} \text{ cm}^{-3}$  and annealed at 900 °C in N<sub>2</sub>, obtained by integrating the PL spectra measured by exciting in the 260-370 nm wavelength range.

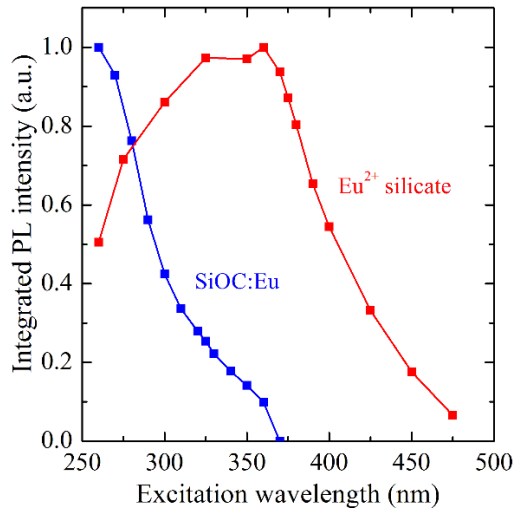


Fig. 7. Comparison of the room temperature PLE spectra of Eu-doped SiOC annealed at 900 °C in N<sub>2</sub> (obtained by integrating the PL spectra measured by exciting with wavelengths in the range 260-370 nm) and of an Eu<sup>2+</sup> silicate (obtained by integrating the PL spectra measured by exciting with wavelengths in the range 260-475 nm). The two spectra are normalized.

From the comparison with the PLE spectrum of an Eu<sup>2+</sup> silicate [16], reported in the same figure, it is evident that the PL efficiency of Eu-doped SiOC is strongly enhanced for wavelengths  $\leq 300$  nm; indeed, its PLE curve is characterized a monotonic decrease by increasing the excitation wavelength, while the Eu<sup>2+</sup> silicate exhibits a maximum at about 350 nm and it is remarkably less efficient for shorter excitation wavelengths, in agreement with

literature data concerning very different  $\text{Eu}^{2+}$ -containing systems [31–33]. Since, as shown in Fig. 4, also the PLE spectrum of undoped SiOC monotonically decreases by increasing the excitation wavelength, it is possible to conclude that the SiOC matrix has an active role in the optical properties of Eu-doped SiOC. We can reasonably exclude that this role consists in the presence of a SiOC emission, since the spectral shape shown in Fig. 6 for an excitation wavelength of 325 nm does not appreciably change by changing the excitation wavelength, even by using the wavelengths which maximize a possible SiOC emission. We could therefore suppose the existence of an energy transfer mechanism, in which the very efficient absorption properties of SiOC in the short wavelength region are exploited to transfer the excitation energy to the  $\text{Eu}^{2+}$  ions, by enhancing their PL efficiency under excitation at short wavelength.

Further information about the nature of  $\text{Eu}^{2+}$  emission can be obtained by time-resolved PL measurements. Figure 8 shows the time-decay curves of an Eu-doped SiOC sample with an Eu concentration of  $1.5 \times 10^{20} \text{ cm}^{-3}$  and treated at 900 °C in  $\text{N}_2$ , measured at different emission wavelengths lying within the broad PL peak shown in Fig. 6.

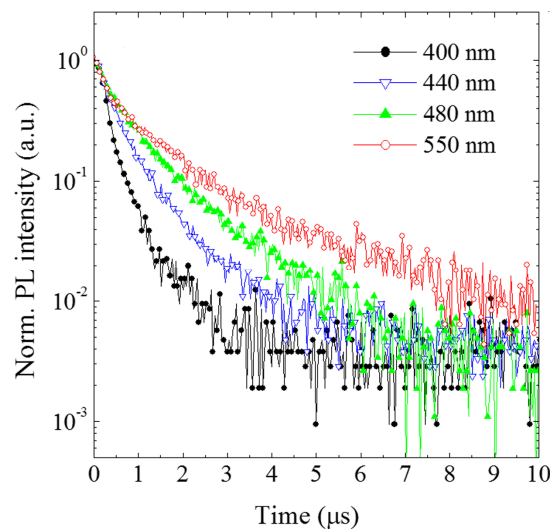


Fig. 8. Room temperature PL time-decay curves of Eu-doped SiOC treated in  $\text{N}_2$  at 900 °C, measured at different emission wavelengths.

All of the curves are not single-exponential. The values of the decay-time  $\tau$ , obtained by taking the time at which the PL signal is  $1/e$  of the value at the laser shut-off, depend on the emission wavelength, since  $\tau$  varies in the range 0.3–0.8  $\mu\text{s}$ . Similarly to the interpretation given to the same phenomenon observed in Si nc [34], the dependence of the  $\tau$  values of the Eu PL emission on the detection wavelength could be due to the mutual interactions among non-equivalent  $\text{Eu}^{2+}$  sites. These sites are characterized by a different local Eu concentration and, in agreement with literature [27], the PL peak is redshifted when the concentration is higher. Sites characterized by a faster decay lifetime show a radiative emission at shorter wavelengths and non-radiative decay channels that quench the PL emission through the interaction with sites emitting at longer wavelengths. On the other hand, sites characterized by very high Eu concentrations (emitting at longer wavelengths) can hardly transfer their energy to other Eu sites and therefore exhibit the longest decay lifetime values. Time resolved PL measurements therefore demonstrate that the  $\text{Eu}^{2+}$  band peaked at 440 nm shown in Fig. 6 can be actually considered the convolution of several contributions, corresponding to different Eu sites in the SiOC matrix.

#### 4. Conclusions

The intense visible emission of SiOC layers has been studied and its dependence on the parameters of the thermal annealing process elucidated. In particular, the presence of two different emitting centers, one related to the presence of Si-C bonds, the other associated to structural defects, has been evidenced and the experimental conditions leading to the prevalence of one contribution with respect to the other have been identified.

Although the emission of SiOC is bright enough to be considered potentially interesting for applications in photonics (as the active medium in Si-based light emitting devices) or in lighting technology, this material has been found to be even more promising as a host matrix for optically active Eu ions. Indeed, Eu precipitation in SiOC is strongly reduced with respect to the more conventional SiO<sub>2</sub> matrix (so greatly increasing the fraction of optically active Eu ions and therefore the optical efficiency of the system) and Eu<sup>3+</sup> ions are efficiently reduced to Eu<sup>2+</sup>, whose very bright visible luminescence is currently attracting a great attention for LED fabrication. Accordingly, our data demonstrate that an increase of the luminescence intensity at 440 nm accounting for about a factor of 15 can be obtained in Eu-doped films in comparison with undoped SiOC. We have also found evidences of the occurrence of an energy transfer mechanism between the matrix and the Eu<sup>2+</sup> ions which, by increasing the efficiency of photon absorption for exciting wavelengths shorter than 300 nm, further contribute to increase the optical efficiency of Eu-doped SiOC layers. These properties open the way to new promising perspectives for the application of Eu-doped materials in photonics and LED fabrication.

#### Acknowledgments

The authors wish to thank F. Priolo and S. Boninelli (MATIS IMM CNR) for fruitful discussions.